Structural and Thermal Analysis of Copper-Doped Poly(*N*-isopropylacrylamide) Films

Sami Makharza[a]; Jihan Auisa[b]; Sawsan Abu Sharkh[c]; Jamal Ghabboun[ad]; Maryam Faroun[a]; Hasan Dweik[b]; Wadie Sultan[b]; Mukhles Sowwan[a]

[a] The Nanotechnology Research Laboratory, Materials Engineering Department, Al-Quds University, East Jerusalem, Palestine [b] Department of Chemistry, Al-Quds University, East Jerusalem, Palestine [c] Biophysics Research Laboratory, Al-Quds University, East Jerusalem, Palestine [d] Department of Physics, Bethlehem University, Bethlehem, Palestine

PLEASE SCROLL DOWN FOR ARTICLE

Taylor & Francis
Taylor & Francis Group

STRUCTURAL AND THERMAL ANALYSIS OF COPPER-DOPED POLY(*N*-ISOPROPYLACRYLAMIDE) FILMS

Sami Makharza,[1] Jihan Auisa,[2] Sawsan Abu Sharkh,[3] Jamal Ghabboun,[1,4] Maryam Faroun,[1] Hasan Dweik,[2] Wadie Sultan,[2] and Mukhles Sowwan[1]

[1]*The Nanotechnology Research Laboratory, Materials Engineering Department, Al-Quds University, East Jerusalem, Palestine*
[2]*Department of Chemistry, Al-Quds University, East Jerusalem, Palestine*
[3]*Biophysics Research Laboratory, Al-Quds University, East Jerusalem, Palestine*
[4]*Department of Physics, Bethlehem University, Bethlehem, Palestine*

In the present study, the chemical structure of thermoresponsive copper-doped poly(N-isopropylacrylamide) thin films was investigated. The polymer thin films were deposited by spin-coating from a solution containing the polymer on silicon windows. Spin-coating was carried out at certain conditions yielding films of nanometric-scale thickness (170–250 mn). Thermal transitions such as low critical solution temperature (LCST) and glass transition temperature (T_g) of polymer samples with respect to copper concentrations were studied by the differential scanning calorimetry (DSC) technique. Thermograms show that thermal transitions shift to higher temperatures after doping polymer with Cu^{+2}. Heat capacity (Cp, Jlg.°C) also increases as the concentration of Cu^{+2} increases. Fourier transform-infrared (FT-IR) spectrum of pure poly(N-isopropylacrylamide) film exhibits several characteristic stretching bands attributed to V_{as} (NH), amide I (C=O), and amide II (C-N) respectively. The infrared spectrum of the corresponding Cu^{+2}-doped polymer thin films showed a significant shift in the characteristic bands compared to that of pure polymer, indicating a strong interaction between Cu^{+2} and poly(N-isopropylacrylamide). The UV-visible spectrum of Cu^{+2}-doped poly(N-isopropylacrylamide) shows the creation of a new band positions at 276 nm and 278 nm. These bands are absent in the pure polymer spectrum, indicating a complex formation between Cu^{+2} and poly(N-isopropylacrylamide). Coil to swollen aggregate formation was investigated by using the tapping mode atomic force microscopy (AFM) technique. Addition of copper ions to the polymer shows a clear change in the morphology of the polymer thin films compared to the morphology of pure poly(N-isopropylacrylamide) prepared with water as solvent, resulting in clusters that approach single nanoparticle behavior.

Keywords: AFM; Poly(*N*-isopropylacrylamide); Polymer metal complex

INTRODUCTION

Poly(*N*-isopropylacrylamide) (PNIPAM) is one of the most stimuli-responsive polymers.[1] It has a lower critical solution temperature (LCST) in water at approximately 32°C.[1,2] PNIPAM has a great potential for applications in biomedical fields,[3–5] switches,[6] and immobilization of enzymes.[7]

PNIPAM chains have a hydrophobic group on the backbone structure. In water solution and below the LCST, the polymer chains are hydrated by the water molecules and form a swollen structure. As the temperature increases above the LCST, hydrogen bonds between the amide groups and the water molecules are suppressed, inducing collapse of the chains.[8] Clusters will be precipitated and formed out of the solution in nanometer-scale size.[9] This effect of PNIPAM-coated surface on substrates offers the ability to control important interfacial phenomena such as wetting,[10,11] fluid flows,[12] adhesion,[13] and the reversible adsorption of biomolecules as a function of temperature.[14]

Different techniques were reported for the preparation of thin PNIPAM films: plasma polymerization,[15] solution casting,[16] layer-by-layer deposition,[17,18] self-assembled monolayers,[19] spin-coating,[20,21] and dip-coating.[22] Spin-coating is an interesting technique commonly used to deposit thin polymer films onto substrates in many fields of polymer preparation and is suited to control film thickness over a wide range. Spin-coating has been applied in many fields of fabrication, such as dielectric layers for microcircuit fabrication[23] and antireflection coatings.[24] Within the present work we apply the spin-coating technique, which is infrequently used for the preparation of PNIPAM thin films.

The Cu (II) ion introduces more packing efficiency to the host, which in turn influences the thermal properties and the morphology of the formed polymer film. The aim of the present work is to study the thermal and surface properties of Cu^{+2}-doped PNIPAM by using differential scanning calorimetry (DSC) and atomic force microscopy (AFM). Moreover, the complex formation was characterized by using Fourier transform-infrared (FT-IR) and ultraviolet-visible (UV-vis) techniques.

As a result of FT-IR and UV-visible spectroscopy, it was found that PNIPAM could coordinate with Cu^{+2} and form the complexes of PNIPAM-Cu^{+2} at different concentrations. DSC results showed a significant change in the lower critical solution temperature and degree of crystallinity of PNIPAM. Surface characterization of PNIPAM and PNIPAM-Cu^{+2} complexes was carried out by using AFM, and the result showed that the surface features of pure PNIPAM below the LCST were significantly different from the surface features of PNIPAM with Cu^{+2} complexes by the formation of clusters when water is used as solvent.

DSC allows the LCST and the degree of crystallinity to be obtained. The peak area was proportional to the enthalpy change in the polymer, and the enthalpy change was related to the amount of crystalline materials present, thus allowing an estimation of the degree of crystallinity. In order to calculate the crystallinity, the enthalpy of fusion for the 100% crystalline material must be known.[25]

EXPERIMENTAL SECTION

Materials and Methods

Poly(*N*-isopropyl acrylamide), copper chloride hexahydrate ($CuCl_2 \cdot 6H_2O$), and absolute ethanol 99% were purchased from Sigma-Aldrich Co. The average molecular weight of PNIPAM is 20–25 KDa. The chemical structure of PNIPAM is shown in Scheme 1. PNIPAM was prepared onto the silicon window through the spin-coating process. For the preparation of 1% (wt/wt) PNIPAM polymer solution, 0.01 g of polymer was dissolved in 1 mL solvent (water or ethanol). Different concentrations of copper solution were prepared. Gradual addition of copper solution to polymer was carried out to obtain 1%, 2.5%, 5%, 7.5%, and 10% wt/wt wt PNIPAM-Cu^{+2} complex formations.

The spin-coating parameters—spin speeds, spin time, and solution concentrations—were controlled to obtain a desired PNIPAM film thickness (250–320 nm). Different concentrations of PNIPAM-Cu^{+2} complexes were prepared (1%, 2.5%, 5%, 7.5%, and 10% wt/wt) and stirred overnight. The solutions were centrifuged for 3 h at 7500 rpm. Thin films were prepared by using the spin-coating method on silicon windows as substrates; the coating was accelerated to 6500 rpm with a time of 40 s to get a thin film of desired thickness. The coated films were dried at 25°C for 1 h to complete removal of solvents.

The silicon window with radius of 1.2 cm is covered completely with the polymer solution. Film thickness is calculated from the density of the solution and the weight of the thin films. The range thickness of sample films can be easily calculated and has been found to be on the nanometric scale.

Instruments

The FT-IR spectra of thin film samples were recorded with a Bruker IFS66/S spectrophotometer.

The NanoDrop ND-1000 spectrophotometer was used to perform the UV-vis spectra. A 1 μL sample was pipetted onto the end of a fiber optic cable (the receiving fiber). A second fiber optic cable (the source fiber) was then brought into contact with the liquid sample, causing the liquid to bridge the gap between the fiber optic ends. Reproducibility was checked for all the samples and no significant differences were observed.

$$\text{[}CH_2 - \underset{\underset{\underset{\underset{\underset{CH_3}{|}}{CH - CH_3}}{|}}{\overset{\overset{\overset{\overset{C=O}{|}}{NH}}{|}}{CH}}\text{]}_n$$
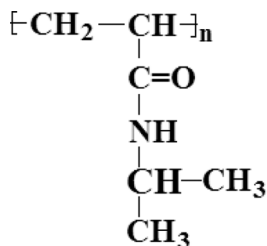
Scheme 1. Chemical structure of PNIPAM.

A scanning atomic force microscope (AFM) and software designed by Nanotech Electronica Company (Madrid, Spain) were used for topographical investigation.[26] A SiN tip with a resonance frequency in the range of 190–325 KHz and force constant in the range of 5.5–22.5 N/m with tip diameter of 10 nm was used as the AFM probe. Tips were purchased from NT-MDT Company (Russia).

Chemat-Technology Spin-Coater KW-4A was used to prepare thin films in the range of nanometric scale thickness.

Thermogram and percent crystallinity of sample thin films samples were obtained by Jade Differential Scanning Calorimetry from PerkinElmer Co.

RESULTS AND DISCUSSION

Figures 1 and 2 represent the FT-IR spectra of the samples in water and EtOH solvent respectively. Table I shows the position of the characteristic bands of PNIPAM and Cu^{+2}-doped PNIPAM in water and ethanol as solvents at different concentrations.

The FT-IR spectrum of pure PNIPAM exhibits three characteristic stretching bands appearing at 3298, 1649, and 1540 cm^{-1}, which have been attributed to V_{as} (NH stretching), amide I (C=O), and amide II (N-H bending) respectively. These vibrations can be influenced by Cu^{+2} doped in the polymer.

The results indicate that there is an interaction between PNIPAM and Cu^{+2}, leading to a decrease in the electron density of nitrogen and oxygen atoms. The interaction between Cu^{+2} and PNIPAM appears through the frequency shift of V_{as} (NH), amide I, and amide II peak positions of pure PNIPAM film. The intensity
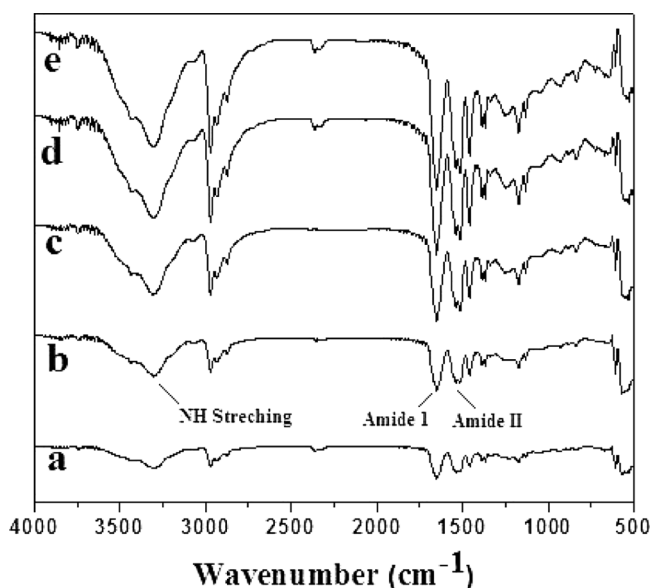
Figure 1. FT-IR spectra of PNIPAM-Cu(II) doped in water solvent at different concentrations: 1%, 2.5%, 5%, 7.5%, and 10%, a–e respectively.
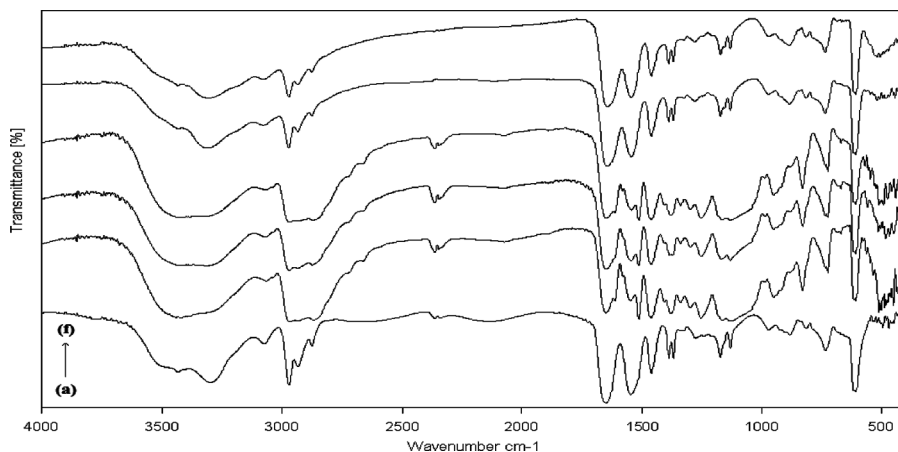
Figure 2. FT-IR spectra of (a) pure PNIPAM film in EtOH solution and (b)–(f) PNIPAM-Cu^{+2} complex films at 1%, 2.5%, 5%, 7.5%, and 10% (wt/wt) respectively.

of the amide I, which is centered at $1649 \, cm^{-1}$, is due to C=O stretching vibration, which is quite sensitive to hydrogen bonding.[28] The interaction between Cu^{+2} and PNIPAM reduces the strength of hydrogen bonding, which causes a decrease in the magnitude of the dipole moment change and results in a less intense carbonyl band.[29] The position of amide I and amide II bands can change with the variation of the conformation of PNIPAM chains in different solvents.[30]

UV-visible spectroscopy provides an accurate and simple method for determining geometry around the transition metal ion in the formation of the polymer complexes.[31]

The optical absorption spectra of PNIPAM and Cu^{+2} solutions in water solvent are shown in Figures 3 and 4, respectively. The UV-vis spectrum of PNIPAM exhibits maximum absorption (λ_{max}) at 228 nm corresponding to π and η electron transition localized on C=O group of PNIPAM. The λ_{max} of Cu^{+2} solution appears at 270 nm. However, in Figure 5, UV-visible results of PNIPAM-Cu^{+2} exhibited an electronic spectrum that differed from the spectrum of both pure polymer and metal

Table I. Characteristic bands of PNIPAM and Cu^{+2}-doped PNIPAM at different concentrations

Band position Sample	V_{as} NH		Amide I		Amide II	
	(a)	(b)	(a)	(b)	(a)	(b)
PNIPAM	3298		1649		1540	
PNIPAM-Cu^{+2} 1%	3302	3297	1648	1650	1541	1515
PNIPAM-Cu^{+2} 2.5%	3306	3294	1648	1648	1543	1519
PNIPAM-Cu^{+2} 5%	3308	3305	1647	1655	1543	1508
PNIPAM-Cu^{+2} 7.5%	3313	3311	1644	1655	1546	1511
PNIPAM-Cu^{+2} 10%	3314	3315	1642	1655	1548	1524

(a) Represents the spectra in EtOH solvent.
(b) Represents the spectra in Water solvent.
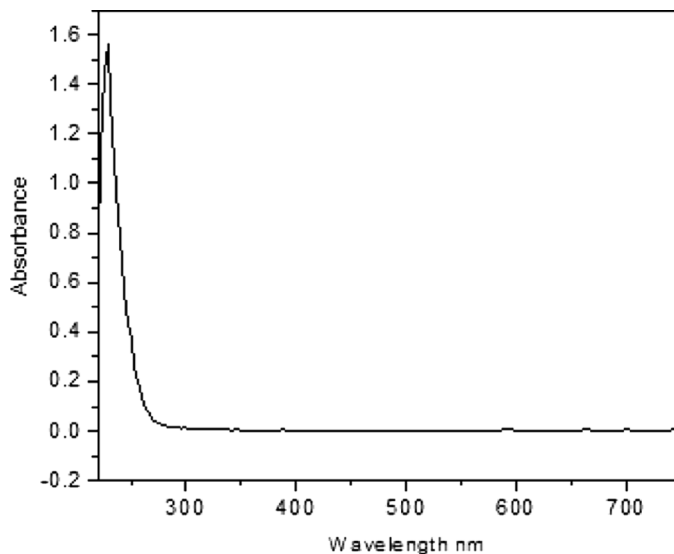
Figure 3. UV visible spectra of PNIPAM solution in water solvent.

solution at different concentrations. The formation of additional new bands at 276 nm and 278 nm confirms the complex formation. The results in EtOH solvent are similar to the results with water solvent.

DSC measurements were performed using PerkinElmer DSC equipment. Samples of about 5 mg, with aluminum pans, nitrogen flow, and a scan rate of 10°C/min were used. The results reported here corresponded to the first heating scan obtained by Cheng et al.[27]

Figure 4. UV-visible spectra of Cu^{+2} solution in water solvent.

Figure 5. UV-visible spectra of PNIPAM-Cu^{+2} at a, 1%; b, 2.5%; c, 5%; d, 7.5%; and e, 10% concentration.
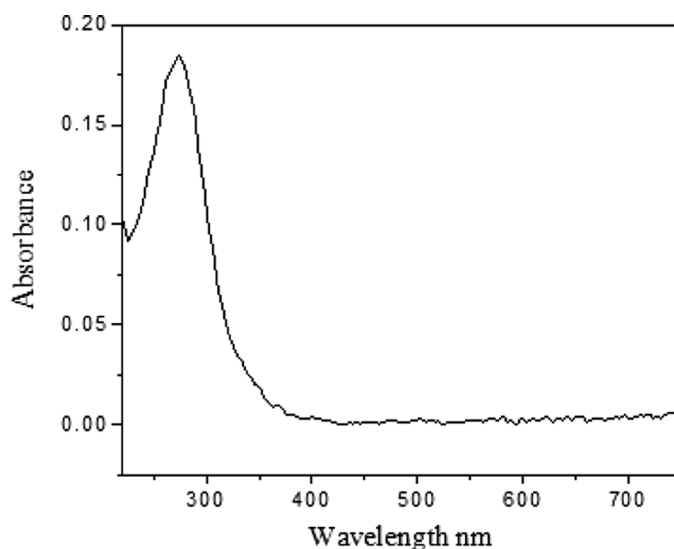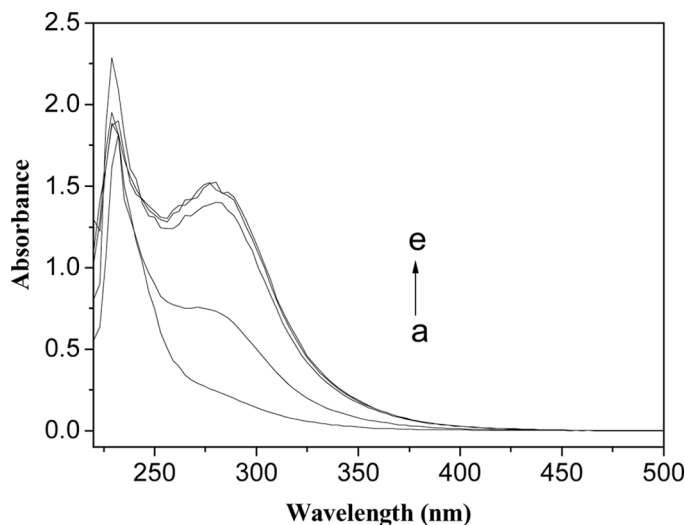
PNIPAM has a glass transition temperature (T$_g$) of 136.9°C.[32] Table II reports the thermal peak positions of pure PNIPAM and the PNIPAM-Cu^{+2} film complexes. Pure PNIPAM film has a low critical solution temperature of 31.2°C and glass transition temperature of 136°C, while the PNIPAM-Cu^{+2} at 5% and 10% shifted in LCST to 32.1°C and 33.8°C respectively, as shown in Figure 6. The enthalpy changes also decreased with increasing Cu^{+2} concentrations.

Figure 7 shows a significant shift in glass transition temperature at 5% and 10% to 138°C and 139°C. This shift is due to a type of interaction that occurs between the hydrophilic part of PNIPAM and Cu^{+2} metal ions. The heat capacity of PNIPAM film increased as the concentration of Cu^{+2} increased.

AFM analysis was performed on the Cu^{+2}-doped PNIPAM thin films adsorbed onto silicon substrates for both solvents, water and ethanol. As can be seen in the AFM images in Figure 8 and in the case of water as solvent, there is a significant difference in the morphology of the film when Cu^{+2} is added to the PNIPAM. As the Cu concentration increases, the probed surface shows that aggregates are formed and are more pronounced with the concentration increase of Cu^{+2}, as shown in Figures 8(a) and (b), to transform into nanoparticle-like behavior at higher Cu

Table II. Thermal peak positions of DSC samples

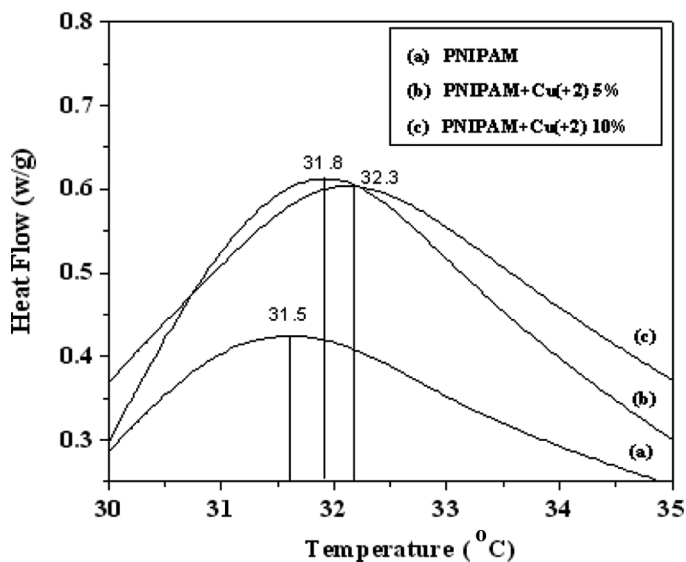| Sample	Peak position^a		Peak position^b	
	LCST (°C)	ΔH (J/g)	T$_g$ (°C)	Cp (J/g)
PNIPAM	31.5	2.06	132.8	0.455
PNIPAM-Cu^{+2} 5%	31.8	2.80	134	0.536
PNIPAM-Cu^{+2} 10%	32.3	3.7	137.6	0.605

Figure 6. DSC thermogram of (a) PNIPAM, (b) PNIPAM-Cu^{+2} (5%), (c) PNIPAM-Cu^{+2} (10%).

concentration. The roughness of the surface increases as well. Representative behavior of the increase in roughness is shown in Figure 8(d), (e), and (f), which are the height cross sections of the AFM images shown in the row above. Figure 9 reveals the effect of ethanol for the high concentration of 20% to 15% of Cu. In the case of ethanol as solvent, AFM images show that the effect of copper is not the same when water is used as solvent (see Figure 9). As the concentration of Cu increases, no aggregates are formed. The cross section of the image in Figure 9(a)
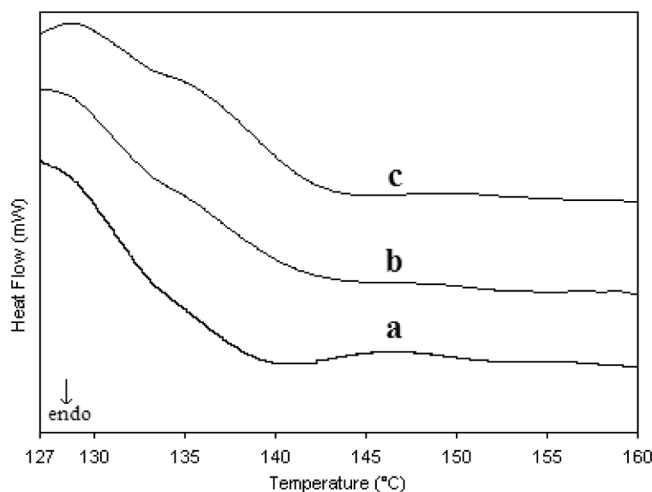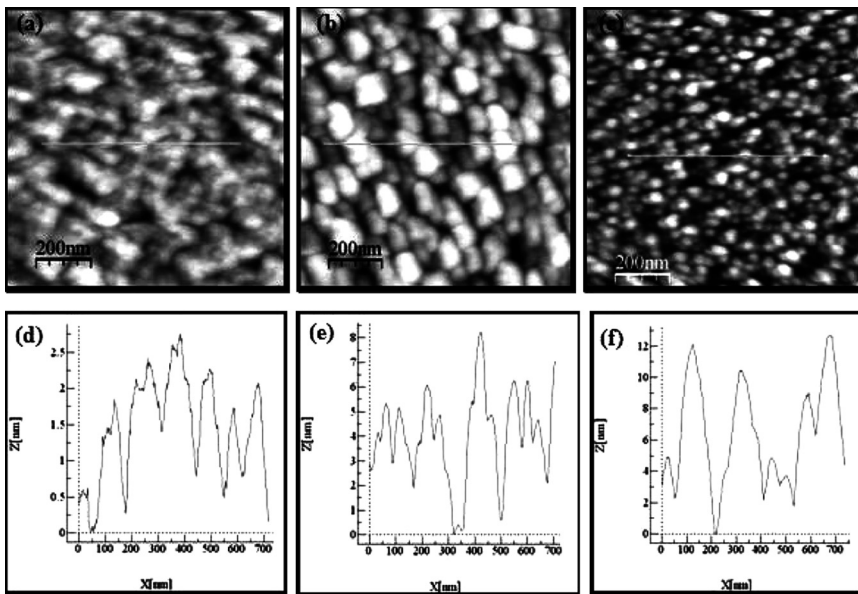

Figure 7. T$_g$ of (a) PNIPAM thin film 1% (wt/wt), (b) PNIPAM-Cu^{+2} at 5%, (c) PNIPAM-Cu^{+2} at 10%.

Figure 8. AFM images of the deposited copper-doped poly (*N*-isopropylacrylamide) thin films on silicon substrates for different concentrations of copper. The polymer is dissolved in water. (a) 1% of Cu^{+2}, (b) 7.5% of Cu^{+2}, (c) 20% of Cu^{+2}. Figures (d), (e), and (f) correspond to the cross-sectional lines for images (a), (b), and (c) in the row above.

is given in Figure 9(b). More data are available for more concentrations, showing the same result for water and ethanol solvents.

Furthermore, current (I) and voltage (V) measurements were performed on the different surfaces with different concentrations of Cu for conductivity investigation. I-V analysis was carried out using the AFM system. Figure 10 shows the I-V curve taken for PNIPAM doped with 20% of Cu^{+2}, indicating the high presence of the metal in the polymer. The I-V curve shows diode-like behavior. No such behavior
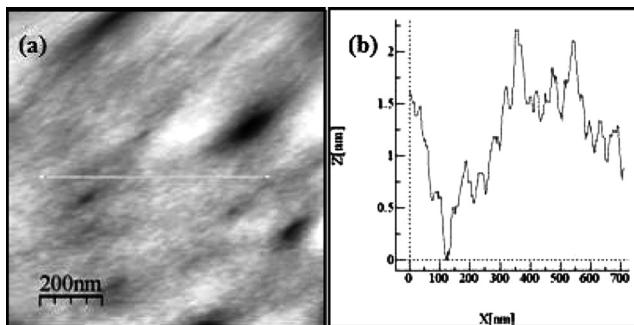
Figure 9. (a) AFM images of the deposited copper-doped poly (*N*-isopropylacrylamide) thin films on silicon substrates for a concentration of 15% copper. The deposited film polymer was dissolved in ethanol. (b) Cross section from AFM image of (a) showing the heights of the formed film.
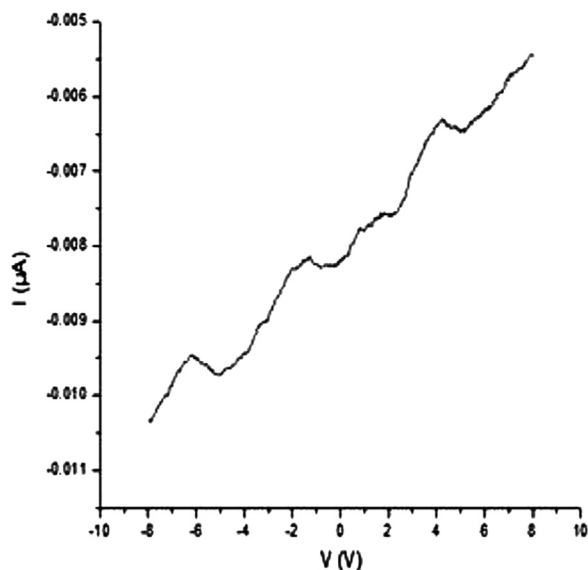
Figure 10. I-V measurement for the Cu-doped PNIPAM with a concentration of 20% of Cu.

has been observed for the surfaces deposited from the ethanol solvent at all concentrations of Cu^{+2} or even at low concentration of Cu^{+2} when water was used as solvent.

CONCLUSION

PNIPAM doped with Cu^{+2} films were investigated by FT-IR, UV-visible spectroscopy, and DSC. The morphological features of the sample thin films were determined by using AFM. The effect of Cu^{+2} on the hydrophilic side group in the PNIPAM backbone is significant. The thermal properties of PNIPAM (LCST and T$_g$) were improved to some extent with the addition of copper ions. The surface roughness changes as the concentration of copper increases in water solvent. Formation of clusters approaches nanoparticle-like behavior upon copper doping with high concentrations. These results open PNIPAM to wider applications in nanotechnology than previously known.

REFERENCES

1. Zhang, X. Z., and R. X. Zhuo. 2000. Preparation of fast responsive, thermally sensitive poly(N-isopropylacrylamide) gel. *Eur. Polym. J.* 36: 2301–2303.
2. Pelton, R. 2000. Temperature-sensitive aqueous microgels. *Adv. Colloid Interface Sci.* 85: 1–33.
3. Duracher, D., A. Elaissari, F. Mallet, and C. Pichot. 2000. Adsorption of modified HIV-1 capsid p24 protein onto thermosensitive and cationic core-shell poly(styrene)– poly(N-isopropylacrylamide) particles. *Langmuir* 16 (23): 9002–9008.

4. De Groot, C. J., M. J. A. Van Luyn, W. N. E. Van Dijk-Wolthuis, J. A. Cadée, J. A. Plantinga, W. Den Otter, and W. E. Hennick. 2001. In vitro biocompatibility of biodegradable dextran-based hydrogels tested with human fibroblasts. *Biomaterials* 22 (11): 1197–1203.

5. Suzuki, K, T. Yumura, Y. Tanaka, and M. Akashi. 2001. Thermoresponsive release from interpenetrating porous silica–poly(N-isopropylacrylamide) hybrid gels. *J. Control. Release* 75: 183–189.

6. Bae, Y. H., T. Okano, R. Hsu, and S. W. Kim. 1987. Thermosensitive networks based on high molecular weight polyoxyethylene and N-isopropylacrylamide. *Makromol. Chem. Rapid Commun.* 8 (10): 481.

7. Liu, F., G. L. Tao, and R. X. Zhuo. 1993. Preparation and properties of poly(*N*-isopropylacrylamide)/poly(*N*-isopropylacrylamide) interpenetrating polymer networks for drug delivery. *Polym. J.* 25: 561.

8. Aseyev, V., H. Tenhu, and F. M. Winnik. In press. In *Self-Organization of Amphiphilic Copolymers in Aqueous Media*, ed. A. R. Khokhlov. Heidelberg: Springer-Verlag.

9. Shoseyov, O., and I. Levy. 2007. *NanoBioTechnology: Bioinspired Devices and Materials of the Future*. Totowa, N.J.: Humana Press.

10. Xia, Y., D. Qin, and Y. D. Yin. 2001. Surface patterning and its application in wetting/dewetting studies. *Curr. Opin. Colloid Interface Sci.* 6: 54.

11. Lenz, P. 1999. Wetting phenomena on structured surfaces. *Adv. Mater.* 11: 1531.

12. Kataoka, D. E., and S. M. Troian. 1999. Patterning liquid flow on the microscopic scale. *Nature* 402: 794.

13. Callow, M. E., J. A. Callow, L. K. Ista, S. E. Coleman, A. C. Nolasco, and G. P. Lopez. 2000. Use of self-assembled monolayers of different wettabilities to study surface selection and primary adhesion processes of green algal (Enteromorpha) zoospores. *Appl. Environ. Microbiol.* 66: 3249.

14. Gan, D., and L. A. Lyon. 2002. Multi-functional nanogels. PEG-modification renders collapsed particles hydrophilic. *Macromolecules* 35: 9634.

15. Cheng, X., H. E. Canavan, M. J. Stein, J. R. Hull, S. J. Kweskin, M. S. Wagner, G. A. Somorjai, D. G. Castner, and B. D. Ratner. 2005. Surface chemical and mechanical properties of plasma-polymerized N-isopropylacrylamide. *Langmuir* 21 (17): 7833–7841.

16. Tsuji, S., and H. Kawaguchi. 2005. Thin films prepared from hydrogel microspheres. *Langmuir* 21: 8439–8442.

17. Serpe, M. J., C. D. Jones, and L. A. Lyon. 2003. Layer-by-layer deposition of thermoresponsive microgel thin films. *Langmuir* 19: 8759–8764.

18. Serpe, M. J., and L. A. Lyon. 2004. Chemical oscillation induced periodic swelling and shrinking of a polymeric multilayer investigated with a quartz crystal microbalance. *Chem. Mater.* 16: 4373–4380.

19. Mangeney, C., F. Ferrage, I. Aujard, V. Marchi-Artzner, L. Jullien, O. Ouari, E. D. Rékaï, A. Laschewsky, I. Vikholm, and J. W. Sadowski. 2002. Synthesis and properties of water-soluble gold colloids covalently derivatized with neutral polymer monolayers. *J. Am. Chem. Soc.* 124: 5811.

20. Hirata, I., M. Okazaki, and H. Iwata. 2004. Simple method for preparation of ultra-thin poly(*N*-isopropylacrylamide) hydrogel layers and characterization of their thermo-responsive properties. *Polymer* 45: 5569–5578.

21. Nykanen, A., M. Nuopponen, A. Laukkanen, S.-P. Hirvonen, M. Rytela, O. Turunen, H. Tenhu, R. Mezzenga, O. Ikkala, and J. Ruokolainen. 2007. Phase behavior and temperature-responsive molecular filters based on self-assembly of polystyrene-*block*-poly(N-isopropylacrylamide)-*block*-polystyrene. *Macromolecules* 40: 5827–5834.

22. You, Y.-Z., Q.-H. Zhou, D. S. Manickam, L. Wan, G.-Z. Mao, and D. Oupicky. 2007. Responsive multiblock copolymers via RAFT polymerization: Synthesis of

temperature- and redox-responsive copolymers of PNIPAM and PDMAEMA. *Macromolecules* 40: 8617–8624.

23. Frank, C. W., V. Rao, M. M. Despotopoulou, R. F. W. Pease, W. D. Hinsberg, R. D. Miller, and J. F. Rabolt. 1996. Structure in thin and ultrathin spin-cast polymer films. *Science* 273: 912.

24. Walheim, S., E. Schäffer, J. Mlynek, and U. Steiner. 1999. Surface-induced structure formation of polymer blends on patterned substrates. *Science* 283: 520.

25. Mulder, M. 1996. *Basic Principles of Membrane Technology*, 2nd ed. Boston: Kluwer Academic.

26. Horcas, I., R. Fernandez, J. M. Gomez-Rodriguez, J. Colchero, J. Gomez-Herrero, and A. M. Baro. 2007. A software for scanning probe microscopy and a tool for nanotechnology. *Rev. Sci. Instrum.* 78: 13705–13713.

27. Cheng, H., L. Shen, and C. Wu. 2006. LLS and FTIR studies on the hysteresis in association and dissociation of poly(*N*-isopropylacrylamide) chains in water. *Macromolecules* 39: 2325–2329.

28. Dweik, H., W. Sultan, M. Sowwan, and S. Makharza. 2008. Analysis characterization and some properties of polyacrylamide copper complexes. *Int. J. Polym. Mater.* 57: 228–244.

29. Sun, B., Y. Lin, and P. Wu. 2007. Structure analysis of poly(N-isopropylacrylamide) using near-infrared spectroscopy and generalized two-dimensional correlation infrared spectroscopy. *Appl. Spectrosc.* 61 (7): 765–771.

30. Liu, M., F. Bian, and F. Sheng. 2005. FTIR study on molecular structure of poly(*N*-isopropylacrylamide) in mixed solvent of methanol and water. *Eur. Polym. J.* 41 (2): 283–291.

31. Kurimura, Y. 1990. Processes of deposition and composite film structure. *Adv. Polym. Sci.* 90: 105.

32. Valdir, M., M. E. S. Ribeiro e Silva, N. Barbani, and P. Giusti. 2004. Binary blends based on poly(*N*-isopropylacrylamide): Miscibility studies with PVA, PVP, and PAA. *J. Appl. Polym. Sci.* 92 (2): 743–748.